Study of Copper Electroless Displacement by Ag+; Prospecting for Multilayers Elaboration

Patrick Fricoteaux* and Christophe Simon

D.T.I., E.A. 3083, Université de Reims, B.P. 1039, 51687 Reims Cedex 02, France

Received: June 6, 2005; In Final Form: August 29, 2005

The copper electroless displacement by silver has been studied in the absence of cyanide ions. The investigations have been carried out using a quartz crystal microbalance, and it was shown that the electroless displacement was plainly diffusion-controlled during 1 min. The electrochemical deposition of Cu−Ag multilayers has been achieved using two methods: by displacement reaction and by alternated applied potentials.

1. Introduction

Cu−Ag multilayers have been recently investigated for their mechanical or electrical properties.[1−7] The deposits were mostly prepared by nonchemical methods[1−5] and very few by electrodeposition.[6−8] In these particular cases, the baths employed were always composed with cyanide salts. The technique used was proposed by Tench and White[8] and consists of a periodic displacement method. The less noble metal (Cu) is electroplated with periodic interruption. During the open-circuit times, copper was substituted via electroless displacement by the more noble metal (Ag). The authors explain that the electroless process may go on beyond a few nanometers by Cu^{2+} transport through pores in the growing Ag layer. With Cu−Ni[9] or Cu−Co[10] systems, others authors have shown that the initial rate of the chemical displacement was controlled by the mass transport of the more noble metallic ion. The present work deals with the investigation of the copper displacement by silver in the absence of cyanide. The obtained results were applied to the preparation of Cu−Ag multilayers by the displacement method and by pulsed polarization.

2. Experimental Section

Because silver is the more noble metal, Ag^+ could be reduced alone and the silver layer could be pure, whereas it is not the case for copper because the reduction of Ag^+ takes place simultaneously with the Cu^{2+} reduction. So, to minimize the silver concentration in the copper phase, it was necessary to use a great concentration ratio between the less noble metal (Cu) and the more noble metal (Ag). Generally, the Cu concentration was typically 100 times greater than that of the Ag concentration. The copper concentrations were comprised between 0.1 and 0.5 mol L^{-1} and the silver concentrations were between 10^{-3} and 5×10^{-3} mol L^{-1}. The electrolytic bath was prepared either with nitrate salts (because of the silver precipitation with sulfate or chloride) or by the dissolution of copper and silver oxides with sulfamic acid.

To avoid precipitation, the reference electrode (saturated mercury sulfate electrode noted as SSE) was separated from the electrolytic bath with a salt bridge filled with the electrolyte.

Ethylenediaminetetraacetic acid (EDTA; 0.75 mol L^{-1}) has been used to realize the experiments.

The pH of the solution was adjusted to 9.3 by the addition of NaOH, and the solutions were deoxygenated over a period of 30 min by nitrogen bubbling before each experiment.

A conventional three-electrode cell in a double jacket was used to maintain a constant temperature (30° C) by the circulation of thermostated water.

The mass changes during the electrodeposition or during the displacement process were followed by a Maxtek quartz crystal microbalance (model PM 710). This technique was based on the changes in the resonance frequency of the crystal as a function of deposited mass according to the Sauerbrey equation (eq 1):[11]

$$\Delta f = -k\Delta m \tag{1}$$

where Δf is the resonance frequency variation, k is the calibration constant, and Δm is the mass deposit variation.

The working electrode was gold-coated quartz with an active surface equal to 1.37 cm^2.

3. Results and Discussion

Electrolyte Choice. To choose a suitable electrolyte, we have realized some preliminary experiments with different salts using the rate R corresponding to the instantaneous mass variation (2) calculated according to

$$R = \Delta m/\Delta t \tag{2}$$

where Δt is the interval of time corresponding to the mass deposit variation (Δm).

As the atomic weight and the number of exchange electrons are different between copper and silver, the instantaneous mass deposit variation was not directly proportional to the current value.

If only Ag^+ was reduced, the Faraday law gives

$$I_{Ag} = F\Delta m_{Ag}/\Delta t M_{Ag} = FR/M_{Ag} \tag{3}$$

where I_{Ag} is the instantaneous silver reduction current, F is the Faraday constant, Δm_{Ag} is the silver deposit mass variation, and M_{Ag} is the silver atomic weight.

When silver reduction is limited by diffusion, eq 3 gives eq 4:

$$I_{l,Ag} = FR_{l,Ag}/M_{Ag} \tag{4}$$

where $I_{l,Ag}$ is the limiting instantaneous silver reduction current

* Corresponding author. E-mail address: patrick.fricoteaux@ univ-reims.fr. Tel.: (33) 3 26 91 85 82. Fax: (33) 3 26 91 31 95.
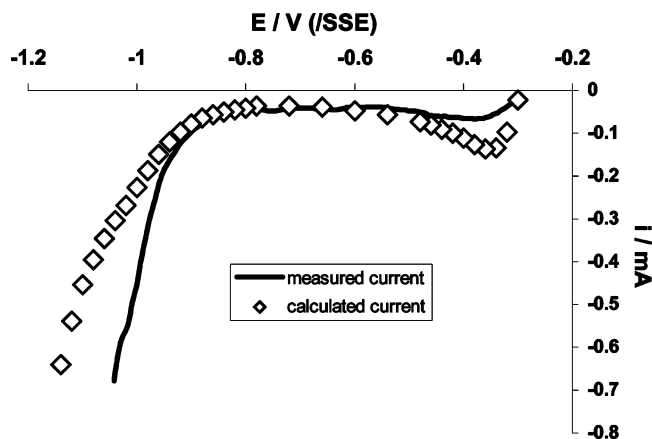
20450 *J. Phys. Chem. B, Vol. 109, No. 43, 2005*

Fricoteaux and Simon

Figure 1. Current vs potential curves obtained with nitrate salts. $[Cu^{2+}]$ = 0.5 mol L^{-1}, $[Ag^+]$ = 0.005 mol L^{-1}, and [EDTA] = 0.75 mol L^{-1}.

and $R_{l,Ag}$ is the limiting rate of mass variation for silver reduction.

Equation 5 below corresponds to the simultaneous silver and copper reduction assuming a 100% mass efficiency.

$$I_t = I_{Ag} + I_{Cu} = (F\Delta m_{Ag}M_{Cu} + 2F\Delta m_{Cu}M_{Ag})/(\Delta t M_{Cu}M_{Ag}) \tag{5}$$

where I_t is the total instantaneous reduction current, I_{Cu} is the instantaneous copper reduction current, M_{Cu} is the copper atomic weight, and Δm_{Cu} is the copper deposit mass variation defined by relation 6.

$$\Delta m_{Cu} = \Delta m - \Delta m_{Ag} \tag{6}$$

Consequently, eq 5 becomes

$$I_t = [F\Delta m_{Ag}M_{Cu} + 2F(\Delta m - \Delta m_{Ag})M_{Ag}]/(\Delta t M_{Cu}M_{Ag}) \tag{7}$$

Considering that copper reduction appears beyond the limiting diffusion of silver, we obtain eq 8:

$$I_t = I_{l,Ag} + I_{Cu} = [FR_{l,Ag}M_{Cu} + 2F(R - R_{l,Ag})M_{Ag}]/M_{Cu}M_{Ag} \tag{8}$$

Finally, the use of the atomic weights and the Faraday constant values allows us to obtain a simple equation to compare directly the instantaneous reduction current with the instantaneous mass variations (eq 9).

$$I_t = 3039R - 2145R_{l,Ag} \tag{9}$$

This equation is valid when copper reduction appears beyond the limiting diffusion of silver and if copper and silver are the only reduced species.

Then, we have realized the intensity−potential curves for different electrolytes using the quartz microbalance as the working electrode (Figures 1 and 2). For each potential, we have simultaneously collected the values of the experimental current (black curves) and the rate values of the mass variations (R). On the silver diffusion stage, we have obtained the value of $R_{l,Ag}$. These values of R and $R_{l,Ag}$ were replaced in eq 9 to calculate the total instantaneous current I_t. Finally, I_t values were plotted as well on Figures 1 and 2. The comparison between the experimental current and the calculated current (I_t) allows us to know if eq 9 is valid, meaning Cu and Ag are the only reduced species.
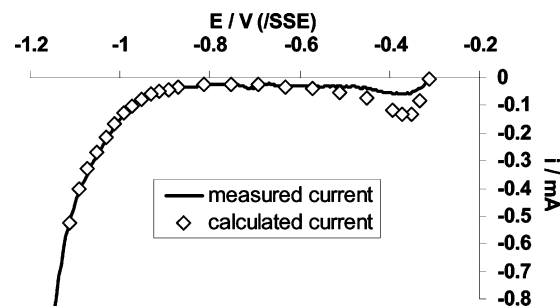

Figure 2. Current vs potential curves obtained with metallic oxides. $[Cu^{2+}]$ = 0.5 mol L^{-1}, $[Ag^+]$ = 0.005 mol L^{-1}, and [EDTA] = 0.75 mol L^{-1}.

The curves were obtained with a scan rate of 2 mV s^{-1}. Three components of curves could be observed in Figure 1. In the first part, the calculated current values are higher to the experimental ones. It means that the mass on the quartz is greater than that obtained by the silver reduction. In the second part, we observe a good fit. It means that the reduction of other species was excluded. Consequently, we attribute the first discordance to adsorption phenomena. These two sectors correspond to the silver reduction. For the third part, the calculated current is lower than the experimental one and corresponds to a mass efficiency different from 100%. This latter occurence was probably due to the nitrate reduction concurrently with the reduction of cupric. Consequently, to verify this hypothesis and to avoid this problem, we had to use an electrolytic bath prepared by the dissolution of copper and silver oxide with sulfamic acid. This time, the calculated curve correctly fits with the experimental one during the copper reduction (Figure 2).

Hence, all the other experiments presented below were realized with this last electrolyte preparation.

Multilayer Preparation by Displacement Reaction. Each time we have realized a copper deposit, the pink color of the deposit was rapidly replaced by a gray color, meaning a displacement reaction between copper and silver occurred.

To check the efficacy of chemical displacement for the multilayer preparation, we tested different concentrations of electroactive species. We plated a 40-nm-thick copper deposit with the chronocoulometry method onto quartz, followed by a rest time of 20 min maximum (or less if 10 nm of silver was deposited by electroless). These sequences were cycled several times, and the mass evolution (during the rest time) was collected versus the time. Then the deposited silver thickness can be calculated.

The applied potential during copper deposition was fixed to −1.4 V/SSE. The corresponding current deposit was sufficiently important to both obtain a good copper purity and obtain a current efficiency equal to 100%.

The silver thickness (eq 13) was calculated according to the mass variation (eq 10), assuming only the following displacement reaction:

$$2Ag^+ + Cu \rightarrow 2Ag + Cu^{2+}$$

$$\Delta m = m_{Ag} - m_{Cu} \tag{10}$$
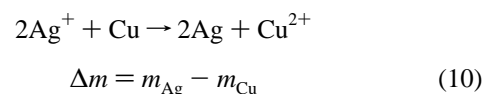
where m_{Ag} is the exchange silver mass and m_{Cu} is the exchange copper mass.

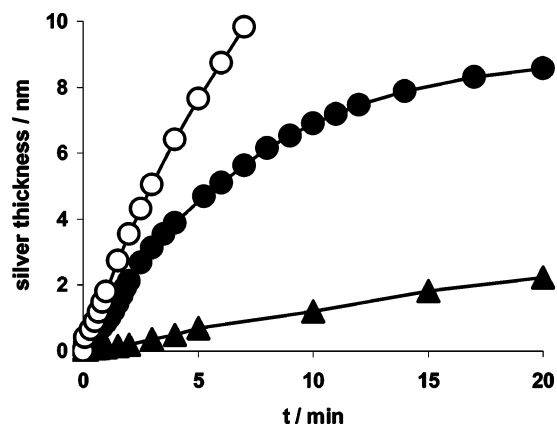When the stoichiometric coefficients of the displacement reaction and the number of silver moles are considered,

Copper Electroless Displacement by Ag⁺

J. Phys. Chem. B, Vol. 109, No. 43, 2005 **20451**

Figure 3. Exchange thickness of silver vs time after 40 nm of copper electrodeposition. ▲, $[Cu^{2+}] = 0.1$ mol L^{-1}, $[Ag^+] = 0.001$ mol L^{-1}, and $[EDTA] = 0.75$ mol L^{-1}; ●, $[Cu^{2+}] = 0.5$ mol L^{-1}, $[Ag^+] = 0.005$ mol L^{-1}, and $[EDTA] = 0.75$ mol L^{-1}; and ○, $[Cu^{2+}] = 0.1$ mol L^{-1}, $[Ag^+] = 0.005$ mol L^{-1}, and $[EDTA] = 0.75$ mol L^{-1}.

eq 10 becomes

$$\Delta m = n_{Ag}(M_{Ag} - 0.5M_{Cu}) \tag{11}$$

where n_{Ag} is the number of exchanged silver moles.

The latter could be replaced by eq 12:

$$n_{Ag} = (\rho_{Ag}Th_{Ag}S)/M_{Ag} \tag{12}$$

where ρ_{Ag} is the silver density, Th_{Ag} is the silver thickness, and S is the deposit area.

The combination of eqs 11 and 12 allows us to obtain the exchange silver thickness (eq 13) from the mass variation detected with the quartz microbalance during the rest time.

$$Th_{Ag} = \Delta m M_{Ag}/[\rho_{Ag}S(M_{Ag} - 0.5M_{Cu})] \tag{13}$$

Figure 3 exhibits the evolution of the exchange silver thickness after a 40-nm copper deposition for different solution concentrations.

With the solution containing 10^{-3} mol L^{-1} of silver, we obtain only 2.2 nm of silver after 20 min. This is attributed to a too small silver concentration in the electrolyte. The multilayer realization with that solution is possible but with a large experiment time. With the other solutions (5×10^{-3} mol L^{-1} silver), the experiment time to obtain 10 nm of silver is acceptable to fabricate multilayers. With the solution containing 0.1 mol L^{-1} copper and 5×10^{-3} mol L^{-1} silver, the experiment time to obtain 10 nm was about 7 min. But, we do not obtain the 10 nm of silver after 20 min (only about 8 nm) with the solution containing 0.5 mol L^{-1} copper. The last phenomenon can be explained by the higher free copper concentration which increases the Nernst potential of the copper system and gets it closer to the silver Nernst potential. The higher free concentration was due first to the increase of copper concentration and second to the decrease of the copper/EDTA ratio.

Then, we checked the reproducibility of the displacement reaction for several cycles with the solution containing 0.1 mol L^{-1} copper and 5×10^{-3} mol L^{-1} silver. The copper deposition was realized by chronocoulometry, while the thickness was controlled by quartz microbalance. The copper deposition time obtained for each cycle was constant and equal to 41 s. In the same manner, the silver exchange was regular with an average of 7 min for 10 nm (Figure 4). The micrography of the deposit obtained after 10 cycles (Figure 5) exhibits a relatively good flatness without dendritic growth.
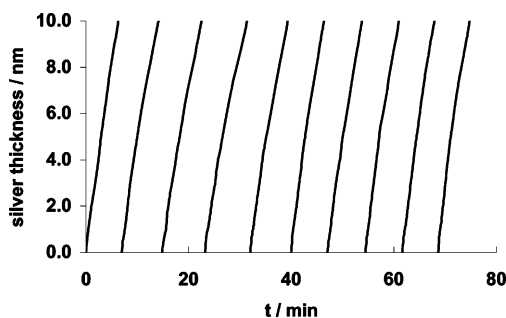

Figure 4. Evolution of the exchange thickness of silver for several cycles. $[Cu^{2+}] = 0.1$ mol L^{-1}, $[Ag^+] = 0.005$ mol L^{-1}, and $[EDTA] = 0.75$ mol L^{-1}.
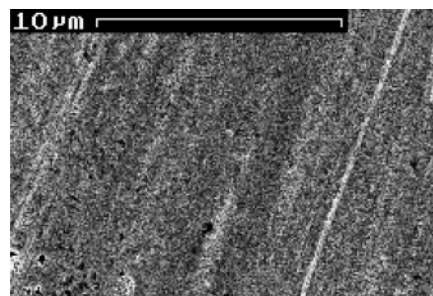

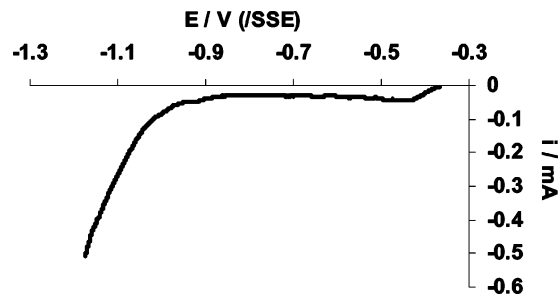**Figure 5.** Scanning electron microscope image of the electroless silver deposit.

Figure 6. Current vs potential curves obtained with metallic oxides. $[Cu^{2+}] = 0.1$ mol L^{-1}, $[Ag^+] = 0.005$ mol L^{-1}, and $[EDTA] = 0.75$ mol L^{-1}.

After the experiment, the deposit was dissolved in nitric acid, and the composition was determined by atomic absorption. The number of silver moles found was equal to 1.17×10^{-6} mol and was in good agreement with the theoretical one found using eq 12 (1.33×10^{-6} mol). This proves that the displacement reaction could be considered as quantitative.

The short time for the chemical exchange (Figure 4) and the good regularity make this solution adequate for multilayer preparation. Note that, during the first minute, the silver exchange thickness variation was linear and equal to 1.8 nm/min. This reaction rate could be limited either by the kinetics of the displacement or by the diffusion of the Ag⁺ ions. Like in ref 10, we have used the Faraday law and the value of the silver deposition limiting current (0.035 mA, Figure 6) to calculate the theoretical deposition rate in the case of Ag⁺ diffusion limitation. The obtained value was equal to 1.6 nm/min for silver electrodeposition, that is, quite close to the experimental one. Consequently, including the experimental errors, we can conclude that the displacement reaction was controlled by Ag⁺ diffusion during the first instants. Afterward, the exchange rate decreases because of the limitation by the Cu²⁺ transport through the pores in the silver layer, as described by Tench and White.[8] Then, the pores are clogged at the same
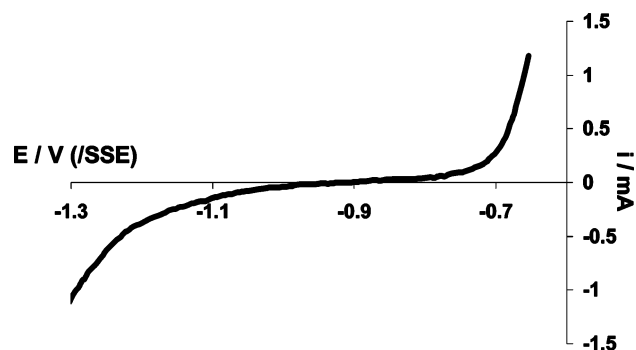
Figure 7. Current vs potential curves obtained with metallic oxides. The scan was realized toward the anodic direction after the copper deposit. Rate sweep = 30 mV s^{-1}. [Cu^{2+}] = 0.1 mol L^{-1}, [Ag$^+$] = 0.005 mol L^{-1}, and [EDTA] = 0.75 mol L^{-1}.
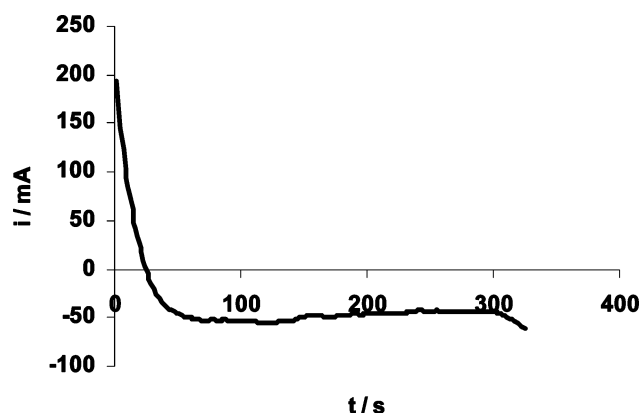
Figure 8. Chronoamperometry curve. Applied potential = −920 mV/SSE. [Cu^{2+}] = 0.1 mol L^{-1}, [Ag$^+$] = 0.005 mol L^{-1}, and [EDTA] = 0.75 mol L^{-1}.

time as the silver layer grows, and it is difficult to obtain a thickness larger than 10 nm by the electroless process.

Multilayer Preparation by Alternated Potential. With systems such as Cu−Ni,[12] it was relatively easy to realize multilayers by applying alternated potentials because the kinetics of the less noble metal (nickel) was slow and no electroless displacement was obtained. It is not the case for the Cu−Ag system because the kinetics of copper (the less noble metal) is quite fast. So, to plate silver while avoiding the copper dissolution, we have to choose a potential at the boundary of the copper oxidation. Figure 7 illustrates the intensity−potential curve obtained with a sweep in the anodic direction after a copper deposit.

We observe the dissolution of copper at about −900 mV/SSE. After different tests, we have defined the following sequence: −1.4 V/SSE during a charge transfer equivalent to −149 mC (i.e., 40 nm of copper) and −920 mV/SSE for −12.9 mC (i.e., theoretically, 10 nm of silver). Note that, with potentials superior to −920 mV/SSE, we obtained a very important copper dissolution. Figure 8 shows the typical response for the silver polarization (−920 mV/SSE).

We observe a slight copper oxidation over a period of about 20 s followed by a reduction current. The final obtained mass variation (detected with quartz microbalance) is equal to 8.8 μg, whereas the theoretical value, according to the Faraday law, should be equal to 14.4 μg (eq 14) considering only the silver reduction. This discrepancy is explained by the simultaneous copper and silver reduction after the phase of copper oxidation. Indeed, if we have only silver deposition and copper oxidation then the mass variation should be higher (see explanation below).
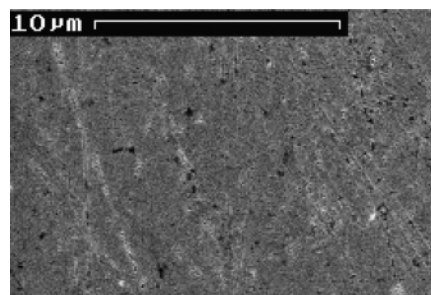

Figure 9. Scanning electron microscope image of the electroplated silver deposit.

If only silver was reduced, the mass variation (eq 14) could be determined versus the silver moles number, $n_{Ag}{}^0$, corresponding to the Faraday law for the charge transfer equivalent to −12.9 mC.

$$\Delta m = n_{Ag}{}^0 M_{Ag} \qquad (14)$$

If silver was reduced simultaneously to the copper oxidation, the mass variation becomes

$$\Delta m = n_{Ag}{}^+ M_{Ag} - n_{Cu}{}^- M_{Cu} \qquad (15)$$

where $n_{Ag}{}^+$ is the number of silver moles reduced and $n_{Cu}{}^-$ is the number of copper moles oxidized.

Given the stoichiometric coefficients and the exchange charges (>0 for oxidation and <0 for reduction), eq 15 gives eq 16 and then eq 17.

$$\Delta m = n_{Ag}{}^0 M_{Ag} + 2 n_{Cu}{}^- M_{Ag} - n_{Cu}{}^- M_{Cu} \qquad (16)$$

$$\Delta m = n_{Ag}{}^0 M_{Ag} + n_{Cu}{}^- (2M_{Ag} - M_{Cu}) \qquad (17)$$

Because the value of $2M_{Ag} - M_{Cu}$ is positive, the mass variation obtained in the presence of copper oxidation should be greater (like with displacement phenomenon) than that obtained with only silver reduction (eq 14). In the same manner, we obtain a mass variation that is inferior if we consider the simultaneous copper and silver reduction (eq 18).

$$\Delta m = n_{Ag}{}^0 M_{Ag} - n_{Cu}{}^- (2M_{Ag} - M_{Cu}) \qquad (18)$$

Therefore, our results show that there was global copper and silver reduction even if, during the first seconds, the chronoamperometry curve (Figure 8) exhibits an oxidation of copper. That could be explained by a displacement of the Nernst potential for the copper system. In fact, just after the copper polarization, the free-copper concentration was very low and the copper equilibrium potential became more negative, allowing the copper oxidation at −920 mV/SSE. Then, the copper concentration increases and the copper equilibrium potential becomes again less negative than −920 mV/SSE.

Let us point out also that the stationary current obtained after 1 min (Figure 8) was higher than the limiting silver reduction current (Figure 6), thus, corroborating the coreduction of copper and silver.

Like after electroless displacement, the deposit was relatively flat (Figure 9). Hence, with this method, we obtain copper−silver multilayers with Cu-rich layers alternated with Ag-rich layers.

4. Conclusion

During this study, we have shown the possibility to realize Cu−Ag multilayers with an electrolyte not containing any

cyanide, according to two methods: displacement reaction and alternated potentials.

With the first method, the silver layer is pure and the electroless kinetics was first controlled by silver diffusion.

In the second one, we obtain a silver layer containing a non-negligible copper quantity.

However, if the silver concentration is too low, the displacement time is quite long but becomes correct with silver concentrations $\geq 5 \times 10^{-3}$ mol L^{-1}.

References and Notes

(1) McKeown, J.; Misra, A.; Kung, H.; Hoagland, R. G.; Nastasi, M. *Scr. Mater.* **2002**, *46*, 593.

(2) Huang, H.; Spaepen, F. *Acta Mater.* **2000**, *48*, 3261.

(3) Soe, W. H.; Kaizuka, T.; Yamamoto, R.; Mitsuhashi, T.; Maekawa, B. S. *J. Magn. Magn. Mater.* **1993**, *126*, 457.

(4) Knoedler, H. L.; Lucas, G. E.; Levi, C. G. *Metall. Mater. Trans. A* **2003**, *34*, 1043.

(5) Czigany, Z.; Kovacs, I.; Radnoczi, G.; Collignon, J. S. *Thin Solid Films* **1998**, *317*, 266.

(6) Ebrahimi, F.; Zhai, Q.; Kong, D. *Mater. Sci. Eng., A* **1998**, *255*, 20.

(7) Tench, D. M.; White, J. T. *J. Mater. Sci.* **1992**, *27*, 526.

(8) Tench, D. M.; White, J. T. *J. Electrochem. Soc.* **1992**, *139*, 443.

(9) Roy, S.; Matlosz, M.; Landolt, D. *J. Electrochem. Soc.* **1994**, *141*, 1509.

(10) Fricoteaux, P.; Douglade, J. *Surf. Coat. Technol.* **2004**, *184*, 63.

(11) Sauerbrey, G. *Z. Phys.* **1959**, *155*, 206.

(12) Wang, L.; Fricoteaux, P.; Yu-Zhang, K.; Troyon, M.; Bonhomme, M.; Douglade, J.; Metrot, A. *Thin Solid Films* **1995**, *261*, 160.